Novel Flapping-wing Micro Aerial Vehicles Utilising Dynamic Amplification

Moonsoo Park
Mechanical Engineering
University College London
London, United Kingdom
ucemmp1@ucl.ac.uk

Ali Abolfathi *
Mechanical Engineering
University College London
London, United Kingdom
a.abolfathi@ucl.ac.uk
*Corresponding author

***Abstract*—This paper introduces a novel design for flapping wing micro aerial vehicles (FWMAVs) that employs dynamic amplification. By utilising mechanical resonance, the design amplifies wing stroke and pitching motions, reducing the energy requirement while enhancing lift production. This approach also minimises the maximum strain on the actuator, thereby improving its structural integrity. A comprehensive mathematical model of the flapping mechanism is developed, incorporating the electromechanical characteristics of piezoelectric materials, nonlinear structural dynamics and aerodynamics. Numerical simulations using MATLAB and Simulink demonstrate the advantages of dynamic amplification, showing a significant improvement in lift generation compared to rigidly structured flapping systems. Using a practical actuator and wing setup, the model predicts a stroke angle of 45 °, a pitching angle of 67 °, a lift generation of 28.4 mN, and average input and output powers of 6.7 mW and 2.9 mW, respectively. This design approach offers a promising pathway for developing high-performance FWMAVs, with potential applications in autonomous flight operations.**

Keywords— Mathematical modelling, dynamic amplification, Flapping wing aerial vehicle, piezoelectric actuator

I. INTRODUCTION

Research into flapping wing micro aerial vehicles (FWMAV) has gotten significant attention in recent few decades [1]. These systems are typically inspired by the flight mechanisms of insects, whose natural designs exhibit remarkable agility and energy efficiency, particularly at small scales. Compared to traditional fixed-wing or rotary-wing designs, bio-inspired FWMAVs offer distinct advantages in manoeuvrability, efficiency and low-speed flight performance, especially in a small size [2]. A piezoelectric actuator is one of the most promising actuators for FWMAVs due to its high power density, linear performance profile, rapid frequency response and controllability [3]. Harvard University [4] and Toyota Central R&D Labs [5] show that piezoelectric unimorph actuators can produce enough lift to make FWMAVs fly.

Accurate estimation and optimisation are essential when designing FWMAVs because the device in millimetre scale typically has low efficiency and the limited power source reduces the flight duration. However, the complexity of a multi-physical system hinders accurate analysis and comprehensive optimisation. Therefore, most studies are conducted based on experiments or focused on isolated parts [6], [7]. Although few studies are developing mathematical models to integrate multidisciplinary systems, they tend to oversimplify the model [8], [9].

In this study, a novel design of a single piezoelectric bimorph actuator-driven FWMAV is developed using a multiphysics modelling approach. The system leverages the superior flight characteristics of insects to enhance its performance. This work provides an in-depth exploration of the system's concept, its key advantages, and the mathematical model developed to analyse and optimise the design. The model investigates the relationships between variables such as electromechanical characteristics of the actuator, flapping kinematics, and flapping wing aerodynamics, offering insights for future FWMAV design. By presenting a mathematical framework for FWMAVs, this research deepens the understanding of the system and provides valuable insight for the future development of highly efficient, resonance-based FWMAVs.

II. DESIGN CONCEPT

The characteristics observed from insect's flight mechanisms that help to produce outstanding flight performance are introduced in [10], [11], [12], [13]. Among key features of insect flight, mechanical resonance, high wingbeat frequency, nearly sinusoidal wing stroke motions, and synchronised wing stroke and pitching motions are considered when designing FWMAV.

In the design, a single piezoelectric biomorph actuator is employed to produce high-frequency reciprocation for flapping motions. Flexural hinges are employed to amplify the limited deformation of the actuator and the system will be driven at its resonant frequency. Additionally, the wing is designed to have a passive pitching motion in accordance with the wing stroke motion. This helps to enhance the lift while it keeps the structure simple. The conceptual design of the FWMAV is shown in Fig. 1.

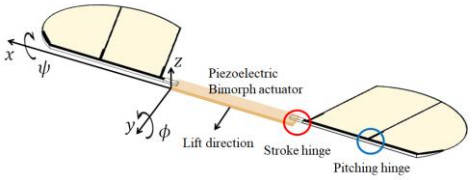

Fig. 1. Design concept and angle definitions for a FWMAV.

A single piezoelectric actuator is represented using a reduced-order model, with the first bending mode assumed to be the dominant motion during flight. This captures the distributed mass, inertia, stiffness and piezoelectric effects of the beam-type actuator. Both stroke and pitching hinges are assumed as rotational stiffnesses while wing load is converted to the combination of wing mass, inertial moment, and aerodynamic forces. The integration of these properties enables the prediction of the mechanical response of the flapping system by an electrical input.

III. Mathematical Modelleing

The developed mathematical model covers the electromechanical characteristics of the piezoelectric actuator, stiffnesses of the stroke and pitching hinges, and aerodynamic load due to passively rotating wings.

A. Aeromechanics of a passively pitching flapping wing

By employing the blade element method, the lift and drag can be formulated as [14],

$$\mathrm{d}L_T = \tfrac{1}{2}\rho u_e^2 C_L(\alpha) c(r) dr \quad (1)$$

$$dD_T = -\mathrm{sgn}(u_e)\tfrac{1}{2}\rho u_e^2 C_D(\alpha) c(r) dr \quad (2)$$

Lift and drag coefficients are [15],

$$C_L(\alpha) = A \sin 2\alpha \quad (3)$$

$$C_D(\alpha) = B - C\cos 2\alpha \quad (4)$$

where A, B, and C are constants determined experimentally.

The angle of attack, α, can be obtained as [16],

$$\alpha = \mathrm{atan2}(\cot(\psi))\,, (-\pi \le \alpha \le \pi) \quad (5)$$

The equation of motions for a passive pitching wing can be obtained by modifying equations in [16] as,

$$J_{xx}\ddot{\psi} = M_x + J_{xy}\ddot{\phi}\cos\psi + \tfrac{1}{2}J_{xx}\dot{\phi}^2 \sin 2\psi - K_\psi \psi \quad (6)$$

where ϕ and ψ are strokes and pitching angles, J_{xx} and J_{xy} are wing inertia tensors ($J_{xx} = \int y^2 dm$, $J_{xy} = \int xy dm$), M_x is the net external moment about the x-axis, K_ψ is the stiffness of the wing hinge around its leading edge. ˙ and ¨ are the first and second time derivatives.

B. Flexural hinges

Flexural hinges are introduced to utilise dynamic amplification for both stroke and pitching angles. The rotational stiffness of the hinges can be determined as [17],

$$K_h = \frac{Y_h t_h^3 w_h}{12 L_h} \quad (7)$$

where Y_h is Young's modulus of the hinge material, t_h, w_h and L_h are the thickness, width and length of the hinge.

C. Actuators

The beam-type piezoelectric actuator is an electromechanical system that produces mechanical deformation in response to the applied electric field. To describe the behaviour of the actuator, the linear constitutive relation is assumed. For a thin beam-type piezoelectric actuator, this linear constitutive relation is expressed as [18],

$$\begin{bmatrix} S_1 \\ D_3 \end{bmatrix} = \begin{bmatrix} s_{11}^E & d_{31}^t \\ d_{31} & \epsilon_{33}^T \end{bmatrix} \begin{bmatrix} T_1 \\ E_3 \end{bmatrix} \quad (8)$$

where *S*, *D*, *T*, and *E* stand for strain, electric displacement, stress and electric field vectors, respectively. s^E is the compliance matrix, ϵ is the permittivity matrix, and d is the dielectric constant matrix. The superscript *E* means that the compliance data was measured under at least a constant, and preferably a zero, electric field. Similarly, the superscript *T* means that the permittivity data was measured under at least a constant, and preferably a zero, stress field and the superscript *t* stands for transpose. Lastly, the numbers 1, 2, and 3 are coincident with the x, y, and z planes.

The equation of motion for the actuator can be represented as [17],

$$\frac{\partial^2 M(x,t)}{\partial x^2} + c_a \frac{\partial w(x,t)}{\partial t} + c_s I \frac{\partial^5 w(x,t)}{\partial x^4 \partial t} + \rho A \frac{\partial^2 w(x,t)}{\partial t^2} = f_e(x,t) \quad (9)$$

where $w(x,t)$ is the lateral displacement of the actuator at the location of x at a time, t, ρA is the length normalised equivalent mass density of the actuator, c_a is the viscous air-damping coefficient, $c_s I$ is the equivalent damping term of the composite cross-section due to structural viscoelasticity, f_e is the external force due to drag.

The bending moment due to the piezoelectric actuator is [19],

$$M(x,t) = YI \frac{\partial^2 w(x,t)}{\partial x^2} + \Theta v(t)[\mathrm{H}(x) - \mathrm{H}(x-L)] \quad (10)$$

where $\mathrm{H}(x)$ is the Heaviside function, $v(t)$ is the input voltage, YI is the bending stiffness of the composite cross-section, and L is the length of the actuator.

The electromechanical coupling coefficient of the piezoelectric actuator is obtained as [19],

Formatted: (none)
Formatted: (none)
Formatted: (none)
Formatted: Font: 10 pt, (none), Ligatures: None

$$\Theta = \left[-\frac{w_a Y_p d_{31}}{t_p}\left(\left(\frac{t_s}{2}+t_p\right)^2-\left(\frac{t_s}{2}\right)^2\right)\right] \quad (11)$$

To confirm the mechanical integrity of the actuator, it is essential to evaluate the maximum strain. Assuming the dominant motion is governed by the actuator's first bending mode, the highest stress occurs at the midpoint of the beam. Consequently, the maximum tensile stress in the actuator can be determined as,

$$\varepsilon_{\max} = \frac{T_{\max}}{Y_p} \quad (12)$$

where Y_p is the Young's modulus of the piezoelectric material and $T_{\max}$ is the tensile stress limit of the material.

In the electrical domain, the electric charge can be determined using Gauss' law. The charge, q_p , in the piezoelectric actuator is expressed as,

$$\nabla \cdot \boldsymbol{D} = q_p = \int_0^t i_p dt \quad (13)$$

The electric charge within the piezoelectric material is generated by both the applied voltage and the dynamic motion of the wing load [19].

$$q_p = q_v + q_d \quad (14)$$

$$q_v(t) = \int_0^{L_a} \frac{\epsilon w_a}{t_p} v_s(t) dx = C_p v_s(t) \quad (15)$$

$$q_d = \int_0^{L_a} d_{31} Y_p \left(\frac{t_s+t_p}{2}\right) w_a \frac{\partial^2 w(x,t)}{\partial x^2} dx = d_{31} Y_p \left(\frac{t_s+t_p}{2}\right) w_a \int_0^{L_a} \frac{\partial^3 w(x,t)}{\partial x^2 \partial t} dx \quad (16)$$

where q_p is the total charge within the piezoelectric material, q_v and q_d are electric charges due to the input voltage and dynamic effect, respectively, ϵ is the permittivity, and C_p is the capacitance of the piezoelectric layer.

The induced current in the piezoelectric bimorph actuator can be obtained as,

$$i_p = 2\frac{dq_p}{dt} \quad (17)$$

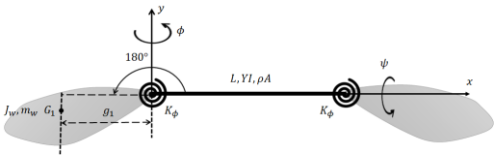

Fig. 2. A schematic view of a FWMAV utilising a single piezoelectric bimorph actuator, where G_1 is the aerodynamic centre of the wing and g_1 is the longitudinal distance between G_1 and the actuator end.

D. System

A simplified diagram for the FMWAV is shown in Fig. 2. The wings are assumed rigid here. The stiffness of the flexural hinge and the mass and inertial moment of the wings are included in boundary conditions while the aerodynamic force is added in the form of external force [20].

Using the separation of variables, expansions theorem and the mode superposition principle [17],

$$w(x,t) = \sum_{n=1}^{\infty} \Phi_n(x)\eta_n(t) \quad (18)$$

where $\Phi_n(x)$ is n^{th} mode shape, and $\eta_n(t)$ is the time-dependent generalised coordinates. In general, the mode shape can be described by [17],

$$\Phi_n(x) = C_{1n}\cos\beta_n x + C_{2n}\sin\beta_n x + C_{3n}\cosh\beta_n x + C_{4n}\sinh\beta_n x \quad (19)$$

$$\beta_n = \sqrt[4]{\frac{\rho A \omega_n^2}{YI}} \quad (20)$$

where ω_n is the resonant frequency and the coefficients, C_{mn} $(m = 1,2,3,4)$, can be determined using force and moment equilibrium at the actuator ends.

The external force due to the aerodynamic force is only applied at the ends of the actuator. The force can be obtained as,

$$f_e(x,t) = -M_{\text{wing}}(x,t)\big|_{x=0,L}\frac{d}{dx}[\delta(x)+\delta(x-L)] \quad (21)$$

The aerodynamic moment due to the flapping motions can be obtained as,

$$M_{\text{wing}}(x,t) = C_w \frac{\partial^2 w(x,t)}{\partial x \partial t}\Big|_{x=0,L}\left|\frac{\partial^2 w(x,t)}{\partial x \partial t}\Big|_{x=0,L}\right| \quad (22)$$

The equations of motion for the system can be rewritten as,

$$\ddot{\eta}_n(t) + 2\zeta_n\omega_n\dot{\eta}_n(t) + \omega_n^2\eta_n(t) = \frac{\Theta v(t)}{\rho A \gamma_n}[\Phi_n'(0) - \Phi_n'(L)] + \frac{1}{\rho A \gamma_n}\left[\Phi_n'(0)M_{\text{wing}}(0,t) + \Phi_n'(L)M_{\text{wing}}(L,t)\right] \quad (23)$$

where $'$ denotes spatial derivative and γ_n is defined as,

$$\gamma_n = \int_0^L \Phi_n^2(x)dx \quad (24)$$

E. Definition of powers and efficiencies

The system is assumed to operate in a hovering condition, where the velocity of the system is zero. Hence drag is used to calculate aerodynamic power. The average electrical input power, P_e, and the averaged aerodynamic power, P_a, can be determined by,

$$P_e = \frac{1}{T}\int_T v(t)i(t)dt \quad (25)$$

$$P_a = \frac{1}{T}\int_T \dot{\phi}\, M_{\text{wing}}(x,t)dt \quad (26)$$

where T is the period of a flapping cycle.

The efficiency of the system, η_s, is calculated as,

$$\eta_s = \frac{P_a}{P_e} \times 100 \quad (27)$$

IV. Simulations

The developed model can predict the mode shape of the system, system resonant frequency, wing stroke angle, pitching angle, energy flows and system efficiency. The numerical solution of the model is obtained using MATLAB and Simulink, with the parameters used for simulation described in TABLE I. While wing specifications are not explicitly defined in this study, wing properties are sourced from [8] where the specification of a manufactured wing is described. The stiffness of the stroke hinge is set to 0.11 mNm/rad which makes the system's natural frequency of about 104 Hz which is the natural frequency of the larger system in [8]. The mode shape of the system is shown in Fig. 3, and the instantaneous responses in the system are illustrated in Fig. 4 to Fig.6. With the current hinge configuration, the actuator's angle is nearly 120 times larger than the actuator's angle, allowing for approximately 45° of wing stroke angle and about 67 ° of pitching angle. The average lift estimation is around 28.4 mN which exceeds the system's weight of approximately 5.3 mN. Lastly, Fig.6 compares the instantaneous input and aerodynamic powers. The average input and aerodynamic powers are 6.7 mW and 2.9 mW, respectively, resulting in a system efficiency of approximately 43 %.

TABLE I. Parameter used for simulations

Parameters	Values	Parameters	Values
V_s	70 V	K_ϕ	1 mNm/rad
L_a	45 mm	K_ψ [a]	86 µNm/rad
t_p	0.152 mm	Y_p	75 GPa
t_s	0.01 mm	Y_s	6.9 GPa
ζ	0.06	ρ_p	7800 kg/m³
L_w [a]	32.4 mm	ρ_s	1370 kg/m³
m_w [a]	4.09 mg	d_{31}	-210 pC/N
J_w [a]	2.7×10^{-10}kg m²	C_p	36 pF
J_{xy} [a]	7.1×10^{-12}kg m²	g_1 [a]	15.6 mm
J_{xx} [a]	1.0×10^{-11}kg m²		

[a] The values are obtained by Ozaki and Hamaguchi and specified in [8]

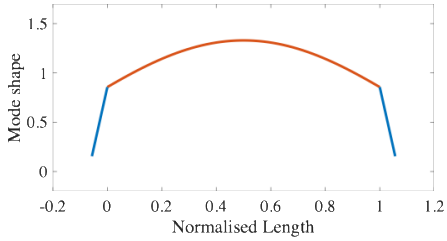

Fig. 3. The first mode shapes of the FWMAV, showing the actuator and wings represented by red and blue lines, respectively. The system's natural frequency is estimated to be 104 Hz, and the length is normalised by the actuator length.

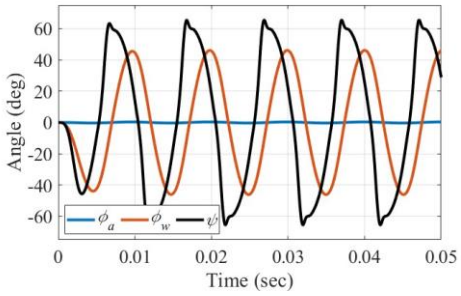

Fig. 4. The estimated instantaneous angles of the FWMAV: ϕ_w is the wing stroke angle, ϕ_a is the angle at the actuator end and ψ is the pitching angle.

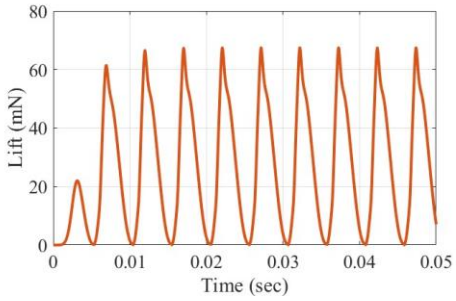

Fig. 5. The estimated instantaneous lift generation of the FWMAV.

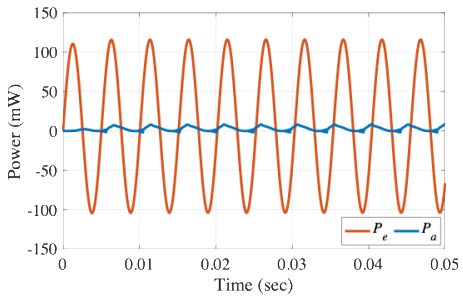

Fig. 6. Instantaneous aerodynamic power, P_a, and input power, P_e.

The wings adopted from previous research may not offer the best performance in this system. Future work will focus on specifying the wing aeromechanics and conducting optimisation to fine-tune the design parameters.

V. Conclusion

In this paper, a novel design concept for flapping wing aerial vehicles that utilises mechanical resonance to achieve enhanced flapping angles and lift. The proposed design aims to mimic the highly efficient natural flight mechanisms of insects by incorporating mechanical resonance and synchronised pitching with flapping motion. This integration enables improved wing stroke angle and energy efficiency. By utilising dynamic amplification, the system can achieve high lift generation with reduced power consumption. The mathematical modelling presented in this study provides a robust framework for understanding the dynamic behaviour of the system. Through deriving and numerically solving the governing equations, the model predicts the stroke angle of 45 °, pitching angle of 67 °, lift generation of 28.4 mN, average input and output powers of 6.7 mW and 2.9 mW, respectively. The theoretical insights gained from this modelling serve as a foundation for future experimental work and optimisation of the design. Overall, this research contributes to the growing field of biomimetic flight systems by offering an innovative approach to FWMAV design that combines the advantages of mechanical resonance. Future work will focus on refining the model, performing empirical validation, and exploring potential real-world applications for this emerging technology.

References

[1] S. Xiao, K. Hu, B. Huang, H. Deng, and X. Ding, "A Review of Research on the Mechanical Design of Hoverable Flapping Wing Micro-Air Vehicles," *J Bionic Eng*, vol. 18, no. 6, pp. 1235–1254, Nov. 2021, doi: 10.1007/S42235-021-00118-4/FIGURES/6.

[2] G. Sachs, "Comparison of Power Requirements: Flapping vs. Fixed Wing Vehicles," *Aerospace 2016, Vol. 3, Page 31*, vol. 3, no. 4, p. 31, Sep. 2016, doi: 10.3390/AEROSPACE3040031.

[3] Alexander H. Slocum, *Precision Machine design*. NJ, 1992.

[4] E. F. Helbling, S. B. Fuller, and R. J. Wood, "Altitude estimation and control of an insect-scale robot with an onboard proximity sensor," *Springer Proceedings in Advanced Robotics*, vol. 2, pp. 57–69, 2018, doi: 10.1007/978-3-319-51532-8_4.

[5] T. Ozaki and K. Hamaguchi, "Bioinspired Flapping-Wing Robot with Direct-Driven Piezoelectric Actuation and Its Takeoff Demonstration," *IEEE Robot Autom Lett*, vol. 3, no. 4, pp. 4217–4224, Oct. 2018, doi: 10.1109/LRA.2018.2863104.

[6] D. Kumar *et al.*, "Insect-inspired micro air vehicle with nanocomposite flapping wings and flexure joints," *SPIE*, vol. 11376, p. 1137616, Apr. 2020, doi: 10.1117/12.2557471.

[7] M. A. Bidakhvidi, R. Shirzadeh, G. Steenackers, and S. Vanlanduit, "Experimental study of the flow field induced by a resonating piezoelectric flapping wing," *Exp Fluids*, vol. 54, no. 11, pp. 1–16, Dec. 2013, doi: 10.1007/S00348-013-1619-Y/FIGURES/17.

[8] T. Ozaki and K. Hamaguchi, "Electro-aero-mechanical model of piezoelectric direct-driven flapping-wing actuator," *Applied Sciences (Switzerland)*, vol. 8, no. 9, Sep. 2018, doi: 10.3390/APP8091699.

[9] R. Zbikowski, "On aerodynamic modelling of an insect-like flapping wing in hover for micro air vehicles," *Philosophical Transactions of the Royal Society A: Mathematical, Physical and Engineering Sciences*, vol. 360, no. 1791, pp. 273–290, Feb. 2002, doi: 10.1098/RSTA.2001.0930.

[10] D. Campolo, "Motor selection via impedance-matching for driving nonlinearly damped, resonant loads," *Mechatronics*, vol. 20, no. 5, pp. 566–573, Aug. 2010, doi: 10.1016/J.MECHATRONICS.2010.05.008.

[11] L. Schenato, D. Campolo, and S. Sastry, "Controllability issues in flapping flight for biomimetic Micro Aerial Vehicles (MAVs)," *Proceedings of the IEEE Conference on Decision and Control*, vol. 6, pp. 6441–6447, 2003, doi: 10.1109/CDC.2003.1272361.

[12] D. E. Alexander, "On the Wing: Insects, Pterosaurs, Birds, Bats and the Evolution of Animal Flight" , USA, Oxford University Press, 215.

[13] A. J. Bergou, S. Xu, and Z. J. Wang, "Passive wing pitch reversal in insect flight," *J Fluid Mech*, vol. 591, pp. 321–337, 2007, doi: 10.1017/S0022112007008440.

[14] M. R. A. Nabawy and W. J. Crowther, "On the quasi-steady aerodynamics of normal hovering flight part II: model implementation and evaluation," *J R Soc Interface*, vol. 11, no. 94, May 2014, doi: 10.1098/RSIF.2013.1197.

[15] Z. J. Wang, J. M. Birch, and M. H. Dickinson, "Unsteady forces and flows in low Reynolds number hovering flight:two-dimensional computations vs robotic wing experiments," *Journal of Experimental Biology*, vol. 207, no. 3, pp. 449–460, Jan. 2004, doi: 10.1242/JEB.00739.

[16] J. P. Whitney and R. J. Wood, "Aeromechanics of passive rotation in flapping flight," *J Fluid Mech*, vol. 660, pp. 197–220, 2010, doi: 10.1017/S002211201000265X.

[17] S. S. Rao "Mechanical Vibrations", 5th ed, New York, Addison-Wesley, 2011

[18] American National Standards Institute, "IEEE standard on piezoelectricity," 1988.

[19] A. Erturk and D. J. Inman, "A distributed parameter electromechanical model for cantilevered piezoelectric energy harvesters," *Journal of Vibration and Acoustics, Transactions of the ASME*, vol. 130, no. 4, Aug. 2008, doi: 10.1115/1.2890402/439241.

[20] C. L. Kirk and S. M. Wiedemann, "NATURAL FREQUENCIES AND MODE SHAPES OF A FREE–FREE BEAM WITH LARGE END MASSES," *J Sound Vib*, vol. 254, no. 5, pp. 939–949, Jul. 2002, doi: 10.1006/JSVI.2001.4138.

Authors' background (This form is only for submitted manuscript for review) *This form helps us to understand your paper better, the form itself will not be published. **Please delete this form on final papers.** *Title can be chosen from: master student, Phd candidate, assistant professor, lecture, senior lecture, associate professor, full professor.

Your Name	Title*	Affiliation	Research Field	Personal website
Moonsoo Park	PhD	University College London	Dynamic analysis, Bio-inspired robots, Mathematical modelling	-
Ali Abolfathi	Associate professor	University College London	Structural Engineering. Bio-inspired robots, Energy harvesting.	-